



REPORT

Secondary nucleation of monomers on fibril surface dominates α -synuclein aggregation and provides autocatalytic amyloid amplification

Ricardo Gaspar^{1,2}, Georg Meisl³, Alexander K. Buell^{3,4}, Laurence Young⁵, Clemens F. Kaminski⁵, Tuomas P. J. Knowles³, Emma Sparr^{1*} and Sara Linse^{2*}

¹Department of Physical-Chemistry, Lund University, Lund, Sweden

²Department of Biochemistry and Structural Biology, Lund University, Lund, Sweden

³Department of Chemistry, University of Cambridge, Cambridge, UK

⁴Institute of Physical Biology, University of D usseldorf, D usseldorf, Germany

⁵Department of Chemical Engineering and Biotechnology, University of Cambridge, Cambridge, UK

Quarterly Reviews of Biophysics (2017), 50, e6, page 1 of 12 doi:10.1017/S0033583516000172

Abstract. Parkinson's disease (PD) is characterized by proteinaceous aggregates named Lewy Bodies and Lewy Neurites containing α -synuclein fibrils. The underlying aggregation mechanism of this protein is dominated by a secondary process at mildly acidic pH, as in endosomes and other organelles. This effect manifests as a strong acceleration of the aggregation in the presence of seeds and a weak dependence of the aggregation rate on monomer concentration. The molecular mechanism underlying this process could be nucleation of monomers on fibril surfaces or fibril fragmentation. Here, we aim to distinguish between these mechanisms. The nature of the secondary processes was investigated using differential sedimentation analysis, trap and seed experiments, quartz crystal microbalance experiments and super-resolution microscopy. The results identify secondary nucleation of monomers on the fibril surface as the dominant secondary process leading to rapid generation of new aggregates, while no significant contribution from fragmentation was found. The newly generated oligomeric species quickly elongate to further serve as templates for secondary nucleation and this may have important implications in the spreading of PD.

1. Introduction

Protein misfolding and aberrant aggregation processes that elude cellular maintenance mechanisms can result in major disturbances of cellular processes. This may lead to protein aggregation diseases, for example Parkinson's disease (PD), the prevalence of which is increasing (Dobson, 2003). In PD, the formation and deposition of amyloid fibrils by the protein α -synuclein (α -syn) is the pathological hallmark associated with degeneration of dopaminergic neurons in the *substantia nigra* (Fink, 2006), and other brain regions. Neurodegeneration is believed to initiate at

the synapse, and once started, the disease spreads without remission until reaching a terminal phase (Danzer *et al.* 2009; Schulz-Schaeffer, 2010). Cell death appears to result from the aggregation process *per se* or the presence of oligomeric aggregates that impair neurotransmission (Lesn e *et al.* 2006; Shankar *et al.* 2008; Wakabayashi *et al.* 2007; Winner *et al.* 2011). Indeed, toxic forms may arise in a reaction involving both monomeric and fibrillar species (Jan *et al.* 2011), generating oligomers at the fibril surface (Cohen *et al.* 2013).

α -Syn is a natively unfolded 140 amino acid protein that exists abundantly in neuronal cells, where it is located in the proximity of vesicles within the presynaptic terminals (Izawa *et al.* 2012). α -Syn comprises 1% of total cytosolic

* Authors for correspondence: Emma Sparr, Department of Physical-Chemistry, Lund University, Lund, Sweden and Sara Linse, Department of Biochemistry and Structural Biology, Lund University, Lund, Sweden. Email: emma.sparr@fkem1.lu.se and sara.linse@biochemistry.lu.se

protein in the nervous system (Stefanis, 2012) with an estimated intracellular concentration ranging from 30 to 60 μM (Rabe *et al.* 2013). The physiological functions of α -syn are still unclear, but are likely related to vesicle trafficking and release (Bisaglia *et al.* 2009). The onset of PD is also unclear, but has been suggested to be related to α -syn levels above a critical aggregation concentration (Galvagnion *et al.* 2015; Pinotsi *et al.* 2016; Rabe *et al.* 2013). The amyloid fibrils formed from recombinant α -syn *in vitro* are highly similar to those extracted from PD patients in terms of morphology and size (Conway *et al.* 1998). *In vitro* experiments have shown that the aggregation of α -syn is very sensitive to solution conditions, such as temperature (Uversky *et al.* 2001), pH (Buell *et al.* 2014), salt concentration (Munishkina *et al.* 2004) and the presence of cofactors (Ashmad *et al.* 2012). In addition, the presence of surfaces, e.g. air–liquid interface for which α -syn has high affinity, has been shown to influence aggregation kinetics *in vitro* (Campioni *et al.* 2014). The primary nucleation of α -syn can be accelerated by the presence of lipid membranes (Galvagnion *et al.* 2015; Grey *et al.* 2015), surfactant micelles (Giehm & Otzen, 2010) and nanoparticles (Vácha *et al.* 2014). Mechanical agitation enhances fibril fragmentation and increases the air–water interfacial area, which may promote heterogeneous primary nucleation (Campioni *et al.* 2013; Giehm & Otzen, 2010). Quiescent conditions may therefore be preferred in mechanistic studies.

The formation of amyloid fibrils occurs through a nucleation-dependent polymerization reaction. Underlying the macroscopically observable sigmoidal growth curves are several possible microscopic steps occurring simultaneously: primary nucleation of monomers in solution or on surfaces, elongation of fibrils through the addition of

monomers to fibril ends, secondary nucleation of monomers on the surface of already existing fibrils and fibril breakage (Arosio *et al.* 2014; Pinotsi *et al.* 2014). In each case, detailed kinetic studies are needed to reveal the relative importance of these steps. For α -syn, mechanistic studies under quiescent conditions are difficult because homogeneous primary nucleation in bulk solution is undetectably slow, a behavior very different from that observed for many other aggregating proteins, including $A\beta_{42}$ (Arosio *et al.* 2015; Cohen *et al.* 2013), $A\beta_{40}$ (Meisl *et al.* 2014), actin (Oosawa & Asakura, 1975) and some prions (Collins *et al.* 2004; Tanaka *et al.* 2006). Therefore, the initiation of *in vitro* aggregation requires the presence of seeds or other surfaces that enhance nucleation; here we have used pre-formed α -syn fibrils.

2. Outline of the problem

The formation of amyloid fibrils by the intrinsically disordered protein α -syn is a hallmark of PD. There is a correlation between spreading of amyloid and neuronal death. It is therefore of utmost importance to characterize the underlying microscopic steps of the assembly reaction that lead to the conversion of soluble α -syn into its insoluble amyloid fibrils. At mildly acidic pH, mimicking specific cellular environments, such as endosomes and lysosomes, the aggregation of α -syn is greatly accelerated compared with neutral pH, and this effect has been attributed to a strongly pH-dependent autocatalytic process. The molecular mechanism of this process could be nucleation of monomers on fibril surfaces or fibril fragmentation as outlined in Fig. 1. Here, we address the problem of elucidating the α -syn aggregation mechanism, with an aim to distinguish between nucleation on fibril surfaces or fibril fragmentation. We have used seeded aggregation kinetics together with a filter trap assay, differential sedimentation analysis, quartz crystal microbalance studies and two-color super-resolution microscopy using *d*STORM to distinguish between these two possibilities. Our data imply that the secondary process consists of nucleation of monomers on the surfaces of existing fibrils, hence rationalizing the autocatalytic nature of the aggregation process.

3. Results

3.1. Non-seeded aggregation kinetic experiments

α -Syn aggregation is strongly influenced by intrinsic and extrinsic factors. In order to obtain a well-controlled system, all kinetic studies were here performed under quiescent conditions at mildly acidic pH (10 mM MES buffer pH 5.5). To investigate the role of surfaces, reactions starting from monomeric α -syn were monitored in untreated polystyrene (PS) plates as well as non-binding PS plates coated with

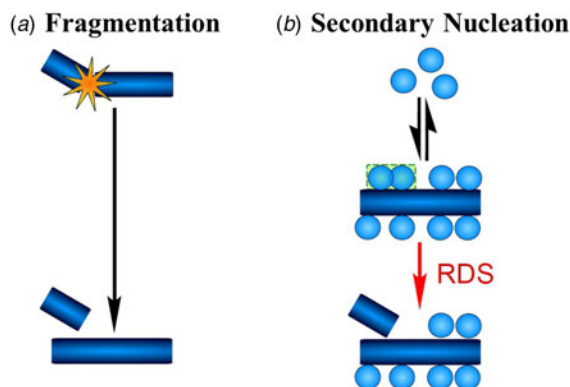


Fig. 1. Schematic depictions of the two possible secondary processes in the aggregation of α -syn at mildly acidic pH conditions. (a) Fibrils multiply through fragmentation. (b) Fibrils catalyze the formation of new aggregates from monomer on their surface. In a saturated secondary nucleation reaction the initial monomer-dependent (attachment) step is so fast that the second monomer-independent (rearrangement or detachment) step becomes the rate determining step (RDS).



polyethylene glycol (PEG). Interestingly, no aggregation of α -syn was detected during the time frame of the experiment (up to 100 h) in the PEGylated plates, whereas reproducible kinetic traces with typical sigmoidal curves were observed in PS plates (S3A). This highlights the importance of heterogeneous nucleation of α -syn on the PS surface as previously found when adding PS nanoparticles to α -syn in the PEGylated plates (Vácha *et al.* 2014). Another striking observation from the current experiments in PS plates is that α -syn aggregation kinetics appear independent of the peptide concentration at high monomer concentrations (above ca. 30 μ M, S3B). To characterize the aggregation mechanism of α -syn in the absence of catalyzing foreign surfaces, all further experiments presented here were conducted in non-binding PEGylated plates in the presence of seeds.

3.2. Seeded kinetic experiments

It is well established that by using preformed fibrils as seeds, the primary nucleation reaction can be bypassed (Buell *et al.* 2014; Giehm & Otzen, 2010). Therefore, the reaction was here monitored in the presence of controlled amounts of α -syn seeds. As the reaction is very sensitive to the concentration and size of the seeds, it is vital to handle all seed solutions in the same manner, as described in the materials and methods section. Initial seeded kinetic experiments were conducted by systematically varying monomer (1–50 μ M) and seed (0.3–3 μ M) concentrations (Figs 2 and 3). The monomer concentrations fall within the physiologically relevant range (Rabe *et al.* 2013). Strikingly, for each seed concentration, the α -syn aggregation rate appears to be independent of the initial monomer concentration above ca. 10 μ M, as evident from the overlapping curves at early times in Fig. 2a–c. This implies that the processes contributing to the aggregation reaction under these conditions, elongation and secondary nucleation are saturated.

Comparing the kinetic curves at a fixed monomer concentration and varied amount of preformed seeds (Fig. 3), it is clear that increasing concentration of seed fibrils leads to a decrease in lag time, and that no aggregation is observed in the absence of seed fibrils. This behavior is observed at all monomer concentrations studied. The formation of new fibrils is thus strongly enhanced by the presence of seed fibrils, which is the definition of a secondary process (Cohen *et al.* 2012). In addition, most of the aggregation curves have concave shapes, i.e. an accelerating rate of aggregation at early times, indicating the existence of a process that significantly increases the number of growth competent ends (i.e. aggregates) (S5).

A number of kinetic models were globally fitted to the experimental data (Meisl *et al.* 2016a) and only models that include secondary processes were found to produce reasonable fits. There are some remaining deviations that may be due to higher-order assembly events (Buell *et al.* 2014)

not included in the existing model. Simulated macroscopic traces for the case of monomer concentration variation in the presence of 1 μ M seed concentration (experimental data shown in Fig. 2b), for the different kinetic models tested are shown in Fig. 2d–f (Meisl *et al.* 2016a). Two models were most consistent with the data: having either fragmentation or saturated secondary nucleation as the dominant processes of fibril multiplication (Fig. 2e, f). This is manifested in the very weak dependence of the overall aggregation rate on the monomer concentration observed in our seeded kinetic data. We next designed experiments to distinguish between fragmentation and nucleation of monomers on fibril surface as the dominant secondary process.

3.3. Sedimentation analysis of fibril size development

The fragmentation of fibrils would lead to a change in fibril size distribution, even after the monomer concentration has reached the solubility limit (Michaels *et al.* 2015). α -Syn aggregates at different times after the aggregation process was completed were investigated using differential sedimentation analysis (Arosio *et al.* 2016). The method relies on the fact that aggregates of different sizes travel through a sucrose gradient at different speeds. The results show that the retention time profile of the samples remains unaltered over up to 20 days (Fig. 4a), implying that the fragmentation rate is undetectably low under quiescent conditions.

3.4. Trap and seed kinetic experiment

As a further test as to whether fragmentation or surface catalysis are the major sources of new aggregates, a set of experiments, referred to as the trap and seed kinetic approach (Arosio *et al.* 2014) was performed at 37 °C under quiescent conditions (Fig. 4b). Mature fibrils were trapped in low-binding GHP membrane filter plates (Nasir *et al.* 2015) with 200 nm cutoff (retentate), and the flow through was collected in non-binding PEGylated plates (filtrate 1). Purified α -syn monomer at different concentrations or buffer alone was added and incubated with the trapped fibrils for 2 h and again filtered (filtrates 2 and 3, respectively). The aggregation kinetics of filtrates 1, 2 and 3 were followed by ThT fluorescence (Fig. 4b). For filtrate 1, no enhanced fluorescence was detected within the time frame of the experiment (90 h), which indicates that seeds were trapped in the GHP membrane filter, and that any monomer or smaller species in the filtrate are present at too low concentration to give rise to any significant aggregation (Fig. 4B1). This control is relevant to show that the system has reached equilibrium. When 16 μ M of monomeric α -syn was added to wells with filtrate 1, aggregation was detected. This implies that some catalyzing species are present in filtrate 1 (Fig. 4B1). For filtrate 2, sigmoidal ThT fluorescence curves are seen within ca. 15 h at all monomer concentrations (Fig. 4B2). In contrast, no fluorescence increase is observed for filtrated monomer that has been

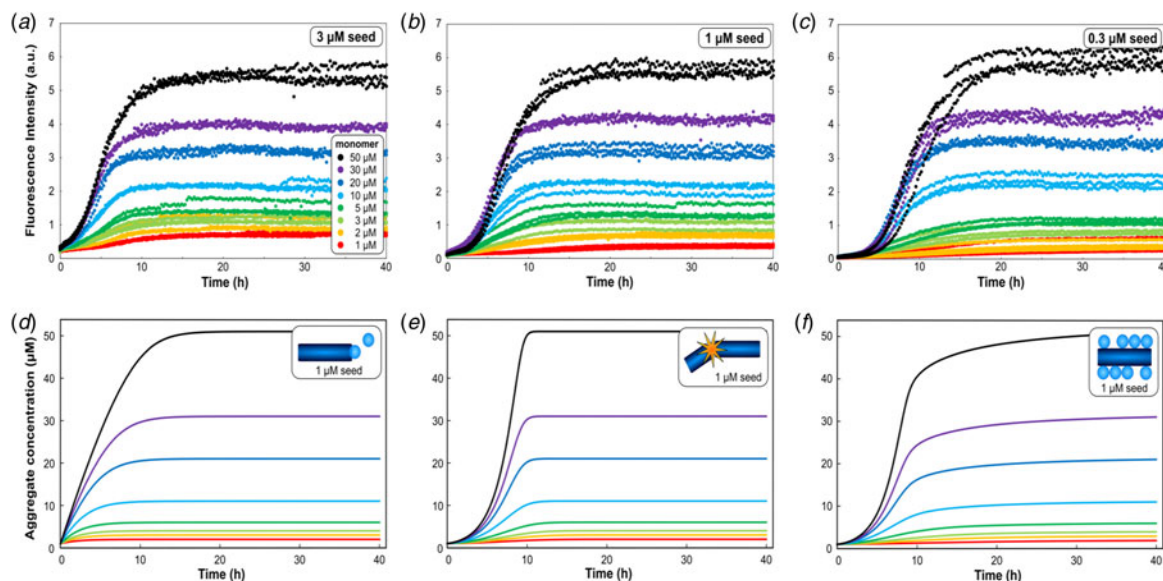


Fig. 2. Seeded α -syn aggregation kinetics. The monomer concentration was systematically varied in the range of 1–50 μ M in the presence of three different seed concentrations: (a) 3 μ M, (b) 1 μ M and (c) 0.3 μ M in 10 mM MES pH 5.5 at 37 $^{\circ}$ C under quiescent conditions. For each solution condition three traces are shown in bold circles. The figures show ThT intensity as a function of time (non-normalized raw data). Different microscopic mechanistic events lead to overall different observable macroscopic kinetic profiles, as shown through simulated traces for the case of monomer concentration variation in the presence of 1 μ M seed (experimental data shown in 2b) for the different kinetic models tested, (d) only primary nucleation and elongation, (e) dominant fragmentation and (f) dominant saturated secondary nucleation.

incubated in the filter plate without seeds (negative control) (Fig. 4B2). Together, this indicates that during incubation of monomer with trapped fibrils, a fibril-catalyzed reaction generates a significant concentration of aggregates that are small enough to pass through the filter together with the remaining monomer. We conclude that the trapped fibrils present catalytic surfaces promoting aggregation of the added monomeric α -syn. ThT was added to filtrate 3 and the fluorescence was monitored for approximately 70 h (Fig. 4B3). The ThT intensity was close to background suggesting either that fibril fragmentation did not occur to any significant extent, or that fragments were larger than the membrane cutoff. After ca. 70 h, 16 μ M monomer was added to filtrate 3, but no fluorescence increase was detected over the following 80 h, confirming the absence of small catalyzing species that could have been present as a result of fibril fragmentation (Fig. 4B3).

3.5. Surface affinity of monomers is pH dependent

The interaction between monomeric and fibrillar α -syn as a function of pH was studied by means of quartz crystal microbalance with dissipation (QCM-D) to monitor the association and dissociation of monomers to and from surface-attached fibrils. This experimental strategy relies on the observation that fibril elongation occurs at significant rates over a much larger pH range than secondary nucleation (Buell *et al.* 2014). The QCM-D measurements provide information on the total amount of adsorbed material

(including the coupled solvent) from the change in frequency (ΔF), as well as the viscoelastic properties of the attached layer from the dissipation (ΔD). Figure 5a shows typical QCM-D data where the decrease in frequency is due to added mass, albeit the relation between frequency and mass addition can be non-linear for viscoelastic layers. Gold coated sensor crystals with covalently immobilized and elongated α -syn fibrils were exposed to 20 μ M α -syn monomer in 10 mM MES buffer at pH 5.5, 5.7, 5.9, 6.1 and 6.5 to allow for monomer adsorption and fibril elongation in different proportions. After a certain frequency shift (\sim 420 Hz) was obtained for each pH condition, each sensor was washed with 10 mM MES buffer pH 6.5 to monitor dissociation. We observe a strong pH dependence of monomer association with the fibrils. A sharp decrease in frequency was observed during incubation with monomer at pH < 6.0, followed by a rapid increase during washing at pH 6.5 (Fig. 5a). This indicates that the majority of mass that was added at pH < 6.0 is reversibly associated. A less sharp decrease in frequency was observed during incubation with monomer at pH > 6.0, followed by a smaller increase during washing, indicating that the majority of the mass added is unaffected by washing at pH 6.5 (Fig. 5a). We interpret this behavior as evidence for two types of mass addition, the relative importance of which depends on the pH. At pH > 6.0 mostly elongation occurs, and monomers are very slowly dissociating upon washing. At pH < 6.0, surface binding becomes significant, and the mass addition is reversible upon washing at pH > 6.0. Therefore, reversible

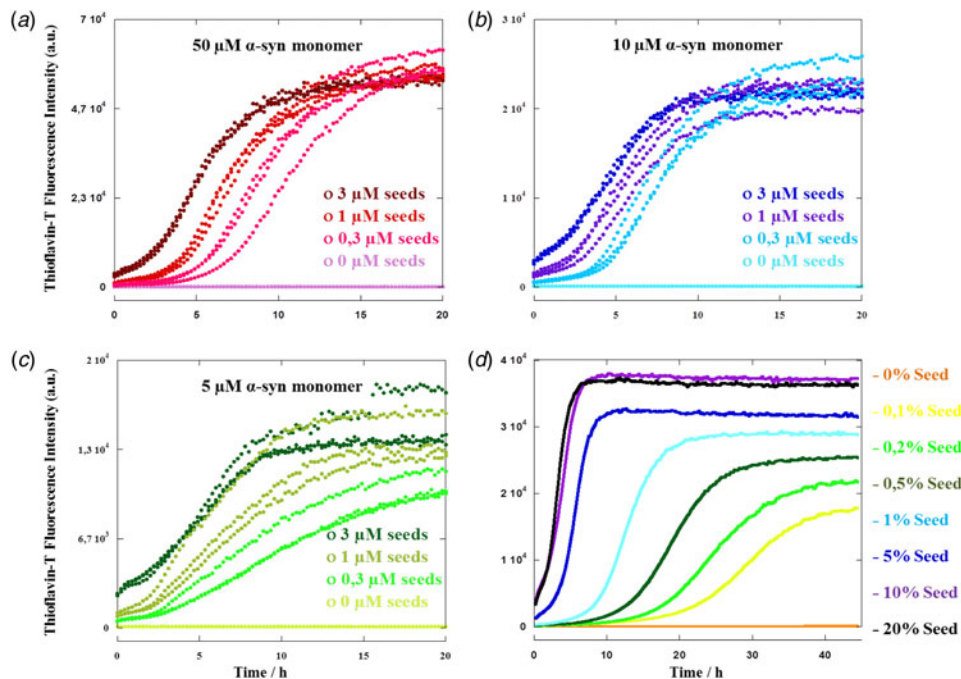


Fig. 3. Seeding efficiency in α -syn aggregation. (a–c) Representative seeded aggregation kinetic traces in the presence of fixed (3, 1, 0.3 and 0 μ M) seed concentrations incubated with (a) 50 μ M, (b) 10 μ M and (c) 5 μ M α -syn monomer. For each condition three traces are shown in bold circles. (d) Aggregation with systematic variation of α -syn seed concentration from 0 to 20% in the presence of a fixed α -syn monomer concentration (20 μ M). Averages of three traces are shown as solid lines. All figures show ThT intensity as a function of time (non-normalized raw data). Therefore, experiments in the presence of seeds show elevated ThT intensity at time zero. All experiments were performed in 10 mM MES pH 5.5 in non-binding PEGylated plates at 37 $^{\circ}$ C and under quiescent conditions.

surface binding has a similar pH dependence as the secondary process (Buell *et al.* 2014), providing additional support for the hypothesis that the secondary process consists of nucleation of monomers on the surface of existing fibrils.

3.6. Imaging of amyloid growth from seed fibrils

In order to investigate amyloid growth from seed fibrils at mildly acidic pH conditions, we imaged samples with super-resolution microscopy. The approach employed was a two-color *d*STORM strategy previously reported (Pinotsi *et al.* 2014). This technique relies on labeling two samples of an α -syn cysteine variant (N122C) with two different Alexa Fluor dyes, namely Alexa Fluor 647 (AF647) and Alexa Fluor 568 (AF568). Preformed seeds of α -syn-AF647 (purple) were incubated with α -syn-AF568 (green) monomer at pH 5.5 (Fig. 6). Comparing with images taken at neutral pH (Pinotsi *et al.* 2014), it is again clear that the aggregation mechanism is pH dependent. Two scenarios were discerned from these images: at mildly acidic pH monomer showed affinity for the surface along the sides of the existing seeds (co-localization of purple and green in Fig. 6), while for neutral pH conditions elongation dominated and monomer showed greater affinity for the growth-competent fibril ends (Pinotsi *et al.* 2014). It should be noted here that, irrespective of the conditions during sample preparation, the *d*STORM imaging was performed in a dedicated imaging

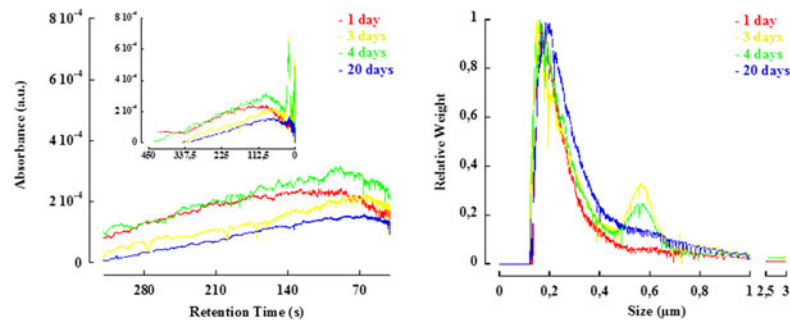
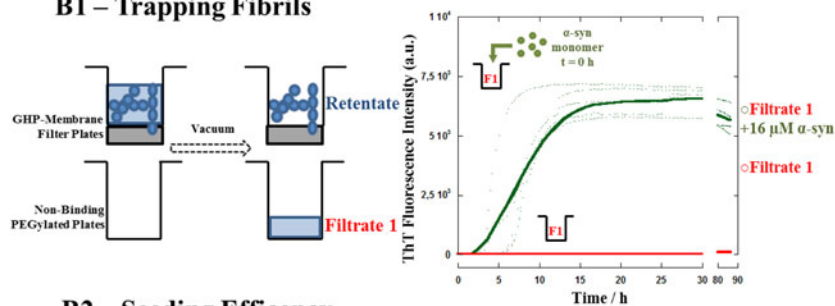
buffer at pH 8.2. As the majority of the mass added at mildly acidic pH is reversibly associated, as inferred from the QCM-D data (Fig. 5), it is likely that the majority of the mass added to the fibril seeds at pH 5.5 detach from the fibrils when they are placed in buffer of higher pH due to repulsive electrostatic interactions. This might then lead to an underestimation of the amount of associated α -syn-AF568 species at the fibril surface. Still, it is evident that the surfaces along the α -syn-AF647 fibrils contain along their length α -syn-AF568 species.

4. Discussion

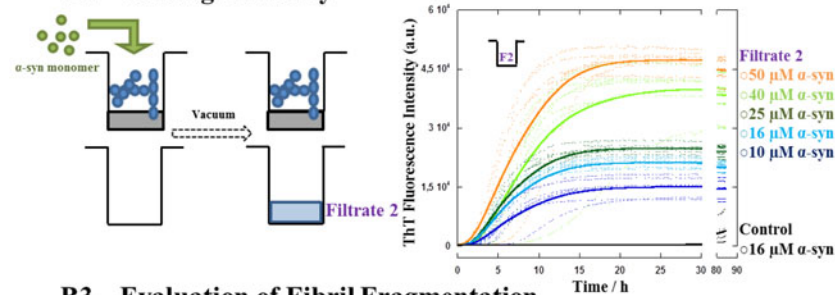
Alterations in the balance of protein synthesis and clearance may lead to the formation of toxic oligomers and trigger a neurodegenerative cascade (Lee *et al.* 2012). No clear correlation has been found between the amount of α -syn inclusions and the stage of PD (Chaudhary *et al.* 2014), although larger areas of the brain contain aggregated α -syn as the disease progresses (Braak *et al.* 2002).

In a previous study, we have shown that the α -syn aggregation is dominated by secondary processes under mildly acidic conditions (pH < 6.0) (Buell *et al.* 2014). It was also shown that at neutral pH, there is a linear relation between the elongation rate and monomer concentration at low monomer concentrations, and that the elongation rate

(a) Differential Sedimentation

(b) Trap and Seed
B1 – Trapping Fibrils

B2 – Seeding Efficiency



B3 – Evaluation of Fibril Fragmentation

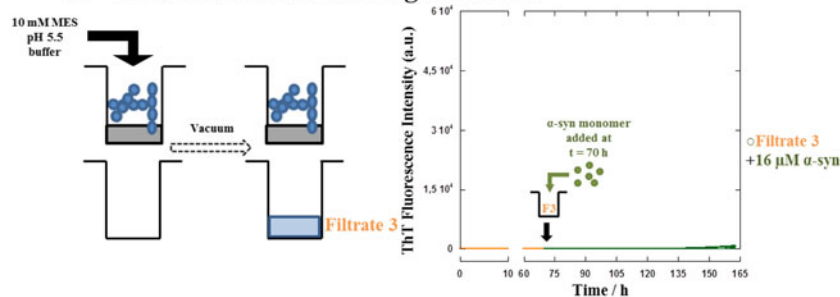


Fig. 4. Experiments designed to identify the dominant secondary process of α -syn aggregation at mildly acidic pH conditions. (a) Time-dependent differential sedimentation analysis performed on fibrils incubated at 37 °C under quiescent conditions in 10 mM MES buffer pH 5.5 for 1–20 days. Aggregates sediment within a sucrose gradient on a rotating disc where longer retention times correspond to smaller size aggregates. The raw data is shown to the left and processed data to the right. The calculations of relative weight and size are made under the assumption of spherical particles, which leads to an underestimation of the size and relative weight for a fibrillar particle. Nevertheless, changes in size distribution can be detected, which was the purpose of this experiment. The figures show representative traces of each condition that was repeated at least two times. (b) Trap and seed kinetic experiment. Fibrils made from 20 μ M α -syn monomer supplemented with 3 μ M seed fibrils in 10 mM MES pH 5.5 were trapped by filtration in filter plates and the flow-through (filtrate 1) was collected in non-binding PEGylated plates, supplemented with ThT and monitored in a plate reader (B1). The trapped fibrils were then incubated for 2 h with concentrations ranging from 10 to 50 μ M α -syn monomer or 10 mM MES buffer pH 5.5 and newly filtered (filtrates 2 and 3, respectively). Again, the flow-through was collected in non-binding PEGylated plates, supplemented with ThT and monitored (B2 and B3). The figures show averages of at least four traces that are shown in bold with individual traces dotted below and are plotted as ThT intensity as a function of time (non-normalized data).

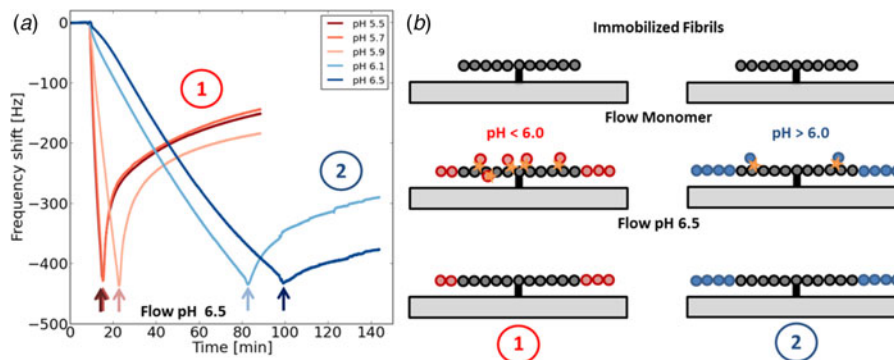


Fig. 5. The surface of α -syn amyloid fibrils shows a pH-dependent affinity for monomeric α -syn. (a) Fibrils of α -syn were immobilized on gold-coated QCM-D sensor crystals and incubated with 20 μ M monomeric α -syn in 10 mM MES buffer at different pH values until a certain frequency shift was reached (ca. -420 Hz for overtone $N=3$). The sensors were then washed with 10 mM MES pH 6.5 (indicated by arrows), leading to different levels of dissociation of the previously attached material. (b) Scheme of what is postulated to occur on the sensors for the conditions of pH < 6.0 and pH > 6.0. The orange stars represent binding to the surface of the fibrils.

becomes saturated at high monomer concentrations (Buell *et al.* 2014). Similar overall behavior has been observed for other amyloid proteins, including Sup35 yeast protein (Collins *et al.* 2004), S6 (Lorenzen *et al.* 2012), insulin (Buell *et al.* 2010a) and α -lactalbumin (Buell *et al.* 2010a).

In the current work, we aim to understand the nature of the dominant secondary process at mildly acidic pH. As a first strategy we studied the monomer dependence of the aggregation kinetics in the presence of low concentrations of pre-formed seed fibrils. Two different scenarios are consistent with the observation that the aggregation kinetics is only weakly dependent on the concentration of monomeric α -syn: (a) fibrils multiply through fragmentation or (b) fibrils catalyze the formation of new aggregates from monomers on their surface, but this reaction is saturated at the monomer concentrations investigated. Secondary nucleation consists of an initial attachment of monomers to the surface, followed by nucleus formation and detachment. However, secondary nucleation may saturate at high enough monomer concentrations, where the initial attachment becomes very fast. The fibril is then fully covered in monomer and the second, monomer-independent (rearrangement or detachment) step, becomes rate limiting (Meisl *et al.* 2014). The two models lead to the same overall scaling of the kinetic behavior with monomer and fibril concentration. To distinguish the nature of the dominant secondary mechanism, additional and complementary experiments were performed including: (i) differential sedimentation, (ii) the trap and seed kinetic approach, (iii) QCM-D biosensing studies and (iv) two-color super-resolution microscopy using dSTORM.

Fragmentation and secondary nucleation mechanisms may lead to different final states. If fragmentation is the dominant mechanism, then the mature fibrils will keep fragmenting even after completion of the aggregation reaction. However, the differential sedimentation analysis shows that the mature fibrils do not become shorter over time,

implying that spontaneous fragmentation occurs very slowly. This makes fragmentation of fibrils less likely to be the dominant secondary mechanism.

The trap and seed kinetic approach was used to probe whether new oligomeric aggregates smaller than 200 nm are formed during a reaction involving both monomer and fibrils. We found that α -syn aggregation is clearly faster in samples of filtrates from reactions where α -syn monomers had been incubated with trapped fibrils compared with samples where α -syn monomers had been incubated for the same time in the same type of filters with no pre-formed seeds, confirming again the importance of secondary processes. Moreover, since shedding/fragmentation of the trapped fibrils when incubated with buffer alone under the same experimental conditions was undetectable, alongside the observation that spontaneous fragmentation does not occur during the time frame studied, we propose that the newly formed oligomeric species are most likely generated by a secondary nucleation process of α -syn monomer at the surface of existing fibrils. As with the seeded kinetic experiments, in the trap and seed assay, we also observed that the aggregation kinetics are to a large extent independent of the monomer concentration, likely a result of saturated secondary nucleation.

QCM-D experiments were set up with changes in pH between the association and dissociation phases to probe whether the added aggregate mass would be reduced at different rates upon washing with buffer at pH 6.5, depending on the pH value during mass association. The QCM-D results reveal that part of the mass associated with the surface-bound fibrils at low pH, dissociates upon pH increase, which is likely due to release of protein that is relatively weakly attached to the surface of the fibrils, i.e. monomeric protein or indeed already formed secondary nuclei. On the other hand, at pH > 6.0 mostly elongation occurs, and monomers dissociate very slowly upon washing due to the high thermodynamic stability

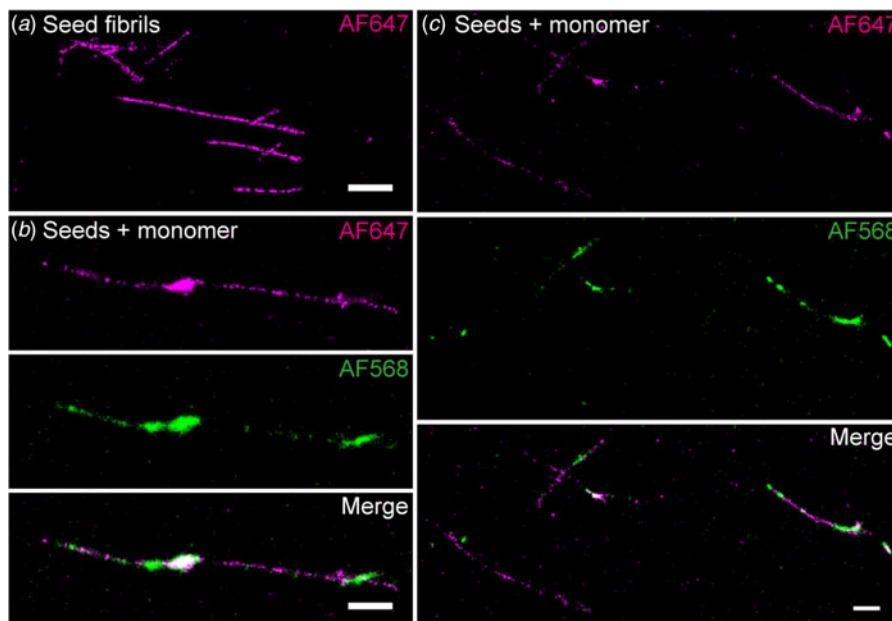


Fig. 6. *d*STORM images of amyloid growth from seed fibrils at mildly acidic pH conditions. (a) Imaged preformed seed fibrils of α -syn N122C labeled with 1:20 AF647 used for the self-seeding experiment. (b, c) α -Syn monomer labeled with AF568 (green) was incubated with 50% seed fibrils labeled with AF647 (purple). The top panel is imaged in the red channel, middle panel imaged in the green channel and the bottom panel is the merge between both channels. Scale bar corresponds to 1 μ m.

of the fibrils (Baldwin *et al.* 2011). The QCM-D experiments, also support that nucleation of new fibrils from surface-bound monomers is the most likely secondary process at mildly acidic pH. The dependence on pH of α -syn monomer surface affinity was also evident in the two-color *d*STORM images. Here, it was clearly shown that at mildly acidic pH conditions, a larger proportion of monomer is bound to the surface along the seed fibrils, opposing to neutral conditions, where monomer has higher affinity for the growth-competent fibril-free ends (Pinotsi *et al.* 2014).

In summary, the combination of experiments presented here very strongly suggests that the nucleation of monomers on fibril surfaces is the secondary process that dominates the aggregation mechanism for α -syn at pH < 6.0. Thus, at mildly acidic pH the aggregation of α -syn follows the same mechanism as previously found for insulin (Foderà *et al.* 2008), IAPP (Padrick & Miranker, 2002) and the amyloid β peptide, A β (Cohen *et al.* 2013; Meisl *et al.* 2014). Although surface catalyzed secondary nucleation dominates the aggregation process for A β also at basic pH, a reduction in pH lowers the electrostatic repulsion between monomers and fibrils leading to enhanced secondary nucleation (Meisl *et al.* 2016b). α -Syn has a pI of 4.7 (Uversky *et al.* 2001) and carries a net negative charge at neutral pH. The sequence is separated into three distinct regions, with a large number of charged residues in the N- and C-terminal regions and a higher fraction of hydrophobic residues in the central region. Interactions involving hydrophobic groups may play a significant role at all pH values, but at neutral pH,

there is significant electrostatic repulsion between monomers, as well as, between monomers and fibrils. The charge of the residues in the termini is modulated by pH and therefore the electrostatic interactions between monomers and fibrils are likely to have strong pH dependence. This may underlie the observed pH dependence of secondary nucleation (Buell *et al.* 2014).

It can be postulated that changes in pH between different cellular environments may affect the rate of formation of potentially cytotoxic oligomeric species, as observed under the conditions studied here. Mildly acidic pH is found in many intracellular compartments, linked to the endocytic and exocytic pathways, making this set of conditions physiologically relevant. *In vitro* studies at mildly acidic pH can thus bring new insights into the microscopic steps underlying the aggregation mechanism of α -syn, and in particular, aggregate multiplication in the brain (Buell *et al.* 2014). The secondary nucleation process of α -syn monomers on fibril surfaces described here is an autocatalytic process, which constitutes a double threat; it increases rapidly both the total load of fibril mass and the amount of smaller oligomeric species that are thought to be the main responsible agents for cytotoxicity (Xue *et al.* 2009). Since secondary nucleation appears as the dominant route to α -syn aggregation at mildly acidic pH, this reaction can be considered a future therapeutic target for development of small molecular inhibitors or using certain chaperones that have been successfully shown to inhibit this specific microscopic process for the A β peptide (Cohen *et al.* 2015).



5. Material and method section

5.1. Recombinant α -syn peptide expression and purification

Human α -syn WT and α -syn cysteine variant (N122C) were expressed and purified using heat treatment, ion exchange and gel filtration chromatography as described previously (Grey *et al.* 2011) (S1). Labeling of α -syn cysteine variant (N122C) with Alexa Fluor 647 and Alexa Fluor 568 was performed as previously reported (Pinotsi *et al.* 2014) (S6).

5.2. ThT kinetic experiments

A key factor in achieving reproducible kinetics is to use pure monomeric α -syn as starting material. Prior to setting up any kinetic measurement, the frozen aliquots were purified with a final size exclusion chromatography run in 10 mM MES pH 5.5 (standard condition) were the central region of the peak is collected in order to assure the presence of only monomeric species (S1). The protein concentration was determined by measuring the UV absorbance at 280 nm and using the extinction coefficient $\epsilon_{280} = 5800 \text{ l mol}^{-1} \text{ cm}^{-1}$. Buffer solutions were filtered and degassed before each run. The isolated monomeric α -syn was always kept on ice to prevent aggregation.

To follow the fibrillation process, samples were aliquoted in 96-well plates with a non-binding surface (black PS plates treated with a PEGylated surface, half-area, 3881 Corning), supplemented with 20 μM of ThT and sealed with a plastic film to avoid evaporation. With the exception being for the experiment to investigate the role of surfaces on α -syn aggregation shown in S3, were also non-treated surface (black PS plates, full volumes, 3631 Costar) were used. The optimal concentration for ThT (20 μM) was accessed to have a linear relationship between fluorescence intensity and aggregate concentration (S2). Plates were incubated at 37 °C up to 100 h in a plate reader (FluoStar Omega or FluoStar Galaxy, BMG Labtech, Offenburg, Germany) under quiescent conditions (excitation filter 440 nm and emission filter 480 nm).

5.3. Preparation of α -syn seed fibrils

α -Syn seed fibrils were formed in Eppendorf tubes (Axygen low-bind tubes) at 37 °C, with low stirring speed (300 rpm) with a teflon bar and left fibrillating for up to 48 h. Parallel kinetic ThT measurements were performed to assure that the plateau was reached during this time period. Before each kinetic experiment, seed fibrils were pre-treated by 1 min continuous sonication at maximum power in a sonicator bath (Struer, Copenhagen, DK) to disperse lumped fibrils. The concentration of seeds is counted as monomer equivalents.

5.4. Differential sedimentation method

In order to measure retention times of the main populations of mature fibrils as a function of time a sedimentation

analysis was performed using a CPS disc centrifuge instrument model DC24000. The instrument was operated at 13 782 rpm and a 4 to 12% sucrose gradient was cast in the spin fluid (Milli-Q water). Dodecane was added last to the gradient to extend its lifetime. Calibration was done with polyvinyl chloride particles with a weight-average diameter of 483 nm, and 100 μl samples were injected.

5.5. Trap and seed

Fibrils were made from 20 μM monomeric α -syn in the presence of 3 μM seeds under quiescent conditions at 37 °C in non-binding PEGylated plates. The fibrils were trapped on the filter membranes (retentate) by filtration applying vacuum for 10 s on a low-binding AcroPrep 96-well filter plate (plate housing – Polypropylene) embedded with a Versatile GH Polypro membrane (GHP – hydrophilic Polypropylene membrane) (Pall Life Sciences, Ann Arbor, MI). The flow through was collected in a 96-well non-binding PEGylated plate (filtrate). The filtration was done using a MultiScreenHTS vacuum (Millipore) manifold. Before loading the seed samples, the GHP filter membrane of the multi-well plate was washed with experimental buffer. The fluorescence intensity of ThT of each filtrate collected in the non-binding PEGylated plates was monitored in a plate reader at 37 °C under quiescent conditions.

5.6. QCM-D measurements

The QCM-D measurements were performed with an E4 instrument (Q-Sense, Västra Frölunda, Sweden). α -Syn fibrils were produced and attached to the gold-coated surface of a quartz sensor (QX301) as previously described (Buell *et al.* 2010b, 2012) (S4). For the main experiments, the sensors were incubated with solutions of 20 μM monomeric α -syn in 10 mM MES buffer at the pH values of 5.5, 5.7, 5.9, 6.1 and 6.5. When the frequency shift had reached approximately 420 Hz in the frequency overtone $N=3$, the sensor surface was washed with 10 mM MES buffer at pH 6.5.

5.7. Two-color super-resolution microscopy using dSTORM

Two-color super-resolution microscopy was performed on an inverted total internal reflectance fluorescence microscope which was custom-built for dSTORM imaging, as described previously (Kaminski Schierle *et al.* 2011; Pinotsi *et al.* 2014). Alexa Fluor 647 and 568 dyes were excited using a 640 nm diode laser (Toptica) and a 561 nm DPSS laser (Oxxius), respectively with an irradiance between 1 and 5 kW cm^{-2} , and a 405 nm laser diode was used as a reactivation source. The fluorescence was collected with a 100X/1.49 NA objective (Nikon) onto an EMCCD camera (iXon3 897, Andor). To induce photo-switching of the dye the fibrils were immersed in a switching buffer consisting of 100 mM mercaptoethylamine (Sigma) in PBS at pH 8.2 supplemented with an oxygen



scavenger to reduce photobleaching (40 mg ml⁻¹ glucose, 50 µg ml⁻¹ glucose oxidase, 1 µg ml⁻¹ catalase). The red and green channels were imaged sequentially, and for each field of view, a series of 10–15 000 frames was acquired with 15 ms exposure time. The acquired dSTORM datasets were analyzed using rapidSTORM 3-3 (Wolter *et al.* 2012) and super-resolution images were generated using a pixel size of 30 nm pixel⁻¹ for both channels. Seeds with different labeling densities were tested for image optimization. Also, these dye labels were evaluated in terms of interfering with the aggregation process using ThT kinetics studies. It was shown that a 1:20 ratio of labeled α -syn to unlabeled peptide was the optimal in terms of labeling density and unperturbed aggregation kinetics (S7).

Supplementary Material

To view supplementary material for this article, please visit <https://doi.org/10.1017/S0033583516000172>

Acknowledgements

This work was supported by the Swedish Research Council and its Linneaus Centers for Organizing Molecular Matter (E. Sparr and S. Linse), the European Research Council (S. Linse), Nanolund (S. Linse), Multipark (S. Linse and R. Gaspar), the Leverhulme Trust (A. Buell), Magdalene College, Cambridge (A. Buell), the Parkinson's and Movement Disorder Foundation (A. Buell), EPSRC (C.F. Kaminski), MRC (C.F. Kaminski) and Wellcome Trust UK (C.F. Kaminski). We thank Gunnel Karlsson for the expert help with Cryo-TEM, C. Galvagnion and C.M. Dobson for kindly providing the plasmid for α -syn cysteine variant (N122C) expression, G. Schierle Kaminski for helpful inputs and discussions concerning the dSTORM experiments and we would also like to acknowledge K. Sanagavarapu, X. Yang, M. Tornqvist, N. Yu and W.Y. Chen for the support given during the dStorm imaging. We also acknowledge T. Cedervall and S. Gunnarsson for expert help with the fibril sedimentation analysis.

Author Contributions

R.G., A.K.B., C.K., T.P.J.K., E.S. and S.L. designed the experiments. R.G., A.K.B. and L.Y. performed the experiments. R. G., A.K.B., G.M., L.Y., T.P.J.K., E.S. and S.L. analyzed data. R. G., E.S. and S.L. wrote the paper. All authors contributed to the manuscript writing and revision.

References

AROSIO, P., CEDERVALL, T., KNOWLES, T. P. J. & LINSE, S. (2016). Analysis of the length distribution of amyloid fibrils by centrifugal sedimentation. *Analytical Biochemistry* **504**, 7–13.

- AROSIO, P., CUKALEVSKI, R., FROHM, B., KNOWLES, T. P. J. & LINSE, S. (2014). Quantification of the concentration of A β 2 propagons during the lag phase by an amyloid chain reaction assay. *Journal of the American Chemical Society* **136**, 219–225.
- AROSIO, P., KNOWLES, T. P. J. & LINSE, S. (2015). On the lag phase in amyloid fibril formation. *Physical Chemistry Chemical Physics* **17**, 7606–7618.
- ASHMAD, B., CHEN, Y. & LAPIDUS, L. J. (2012). Aggregation of α -synuclein is kinetically controlled by intramolecular diffusion. *Proceedings of the National Academy of Sciences of the United States of America* **109**, 2336–2341.
- BALDWIN, A. J., KNOWLES, T. P. J., TARTAGLIA, G. G., FITZPATRICK, A. W., DEVLIN, G. L., SHAMMAS, S. L., WAUDBY, C. A., MOSSUTO, M. F., MEEHAN, S., GRAS, S. L., CHRISTODOULOU, J., ANTHONY-CAHILL, S. J., BARKER, P. D., VENDRUSCOLO, M. & DOBSON, C. M. (2011). Metastability of native proteins and the phenomenon of amyloid formation. *Journal of the American Chemical Society* **133**, 14160–14163.
- BISAGLIA, M., MAMMI, S. & BUBACCO, L. (2009). Structural insights on physiological functions and pathological effects of α -synuclein. *FASEB Journal Review* **23**, 329–340.
- BRAAK, H., TREDICI, K. D., BRATZKE, H., HAMM-CLEMENT, J., SANDMANN-KEIL, D. & RÜB, U. (2002). Staging of the intracerebral inclusion body pathology associated with idiopathic Parkinson's disease (preclinical and clinical stages). *Journal of Neurology* **249** (Suppl. 3), III/1–III/5.
- BUELL, A. K., BLUNDELL, J. R., DOBSON, C. M., WELLAND, M. E., TERENTJEV, E. M. & KNOWLES, T. P. J. (2010a). Frequency factors in a landscape model of filamentous protein aggregation. *Physical Review Letters* **104**, 228101.
- BUELL, A. K., DOBSON, C. M. & WELLAND, M. E. (2012). Measuring the kinetics of amyloid fibril elongation using quartz crystal microbalances. *Methods in Molecular Biology* **849**, 101–119.
- BUELL, A. K., GALVAGNION, C., GASPAR, R., SPARR, E., VENDRUSCOLO, M., KNOWLES, T. P. J., LINSE, S. & DOBSON, C. M. (2014). Solution conditions determine the relative importance of nucleation and growth processes in α -synuclein aggregation. *Proceedings of the National Academy of Sciences of the United States of America* **111**, 7671–7676.
- BUELL, A. K., WHITE, D. A., MEIER, C., WELLAND, M. E., KNOWLES, T. P. J. & DOBSON, C. M. (2010b). Surface attachment of protein fibrils via covalent modification strategies. *Journal of Physical Chemistry B* **114**, 10925–10938.
- CAMPIONI, S., CARRET, G., JORDENS, S., NICOU, L., MEZZENGA, R. & RIEK, R. (2014). The presence of an air-water interface affects formation and elongation of α -synuclein fibrils. *Journal of the American Chemical Society* **136**, 2866–2875.
- CHAUDHARY, H., STEFANOVI, A., SUBRAMANIAM, V. & CLAESSENS, M. (2014). Membrane interactions and fibrillization of α -synuclein play an essential role in membrane disruption. *FEBS Letters* **588**, 4457–4463.
- COHEN, S. I. A., AROSIO, P., PRESTO, J., KURUDENKANDY, F. R., BIVERSTÄL, H., DOLFE, L., DUNNING, C. J., YANG, X., FROHM, B., VENDRUSCOLO, M., JOHANSSON, J., DOBSON, C. M., FISAHN, A., KNOWLES, T. P. J. & LINSE, S. (2015). A molecular chaperone breaks the catalytic cycle that generates toxic A β oligomers. *Nature Structural and Molecular Biology* **22**, 207–213.
- COHEN, S. I. A., LINSE, S., LUHESHI, L. M., HELLSTRAND, E., WHITE, D. A., RAJAN, L., OTZEN, D. E., VENDRUSCOLO, M., DOBSON, C. M. & KNOWLES, T. P. J. (2013). Proliferation of amyloid- β 42 aggregates occurs through a secondary nucleation mechanism. *Proceedings*

- of the National Academy of Sciences of the United States of America **110**, 9758–9763.
- COHEN, S. I. A., VENDRUSCOLO, M., DOBSON, C. M. & KNOWLES, T. P. J. (2012). From macroscopic measurements to microscopic mechanisms of protein aggregation. *Journal of Molecular Biology* **421**, 160–171.
- COLLINS, S. R., DOUGLASS, A., VALE, R. D. & WEISSMAN, J. S. (2004). Mechanism of prion propagation: amyloid growth occurs by monomer addition. *PLoS Biology* **2**, e321.
- CONWAY, K. A., HARPER, J. D. & LANSBURY, P. T. (1998). Accelerated *in vitro* fibril formation by a mutant α -synuclein linked to early-onset Parkinson's disease. *Natural Medicines* **4**, 1318–1320.
- DANZER, K. M., KREBS, S. K., WOLFF, M., BIRK, G. & HENGERER, B. (2009). Seeding induced by α -synuclein oligomers provides evidence for spreading of α -synuclein pathology. *Journal of Neurochemistry* **111**, 192–203.
- DOBSON, C. M. (2003). Protein folding and misfolding. *Nature* **426**, 884–890.
- FINK, A. L. (2006). The aggregation and fibrillation of α -synuclein. *Accounts of Chemical Research* **39**, 628–634.
- FODERA, V., LIBRIZZI, F., GROENING, M., VAN DE WEERT, M. & LEONE, M. (2008). Secondary nucleation and accessible surface in insulin amyloid formation. *Journal of Physical Chemistry B* **112**, 3853–3858.
- GALVAGNION, C., BUELL, A. K., MEISL, G., MICHAELS, T. C. T., VENDRUSCOLO, M., KNOWLES, T. P. J. & DOBSON, C. M. (2015). Lipid vesicles trigger α -synuclein aggregation by stimulating primary nucleation. *Nature Chemical Biology* **11**, 229–234.
- GIEHM, L. & OTZEN, D. E. (2010). Strategies to increase the reproducibility of α -synuclein in plate reader assays. *Analytical Biochemistry* **400**, 270–281.
- GREY, M., DUNNING, C. J., GASPAR, R., GREY, C., BRUNDIN, P., SPARR, E. & LINSE, S. (2015). Acceleration of α -synuclein aggregation by exosomes. *Journal of Biological Chemistry* **290**, 2969–2982.
- GREY, M., LINSE, S., NILSSON, H., BRUNDIN, P. & SPARR, E. (2011). Membrane interaction of α -synuclein in different aggregation states. *Journal of Parkinson's Disease* **1**, 359–371.
- IZAWA, Y., TATENO, H., KAMEDA, H., HIRAKAWA, K., HATO, K., YAGI, H., HONGO, K., MIZOBATA, T. & KAWATA, Y. (2012). Role of C-terminal negative charges and tyrosine residues in fibril formation of α -synuclein. *Brain and Behaviour* **2**, 595–605.
- JAN, A., ADOLFSSON, O., ALLAMAN, I., BUCCARELLO, A., MAGISTRETTI, P. J., PFEIFER, A., MUHS, A. & LASHUEL, H. A. (2011). $A\beta$ 42 neurotoxicity is mediated by ongoing nucleated polymerization process rather than by discrete $A\beta$ 42 species. *Journal of Biological Chemistry* **286**, 8585–8596.
- KAMINSKI SCHIERLE, G. S., VAN DE LIND, S., ERDELY, M., ESBJÖRNER, E. K., KLEIN, T., REES, E., BERTONCINI, C. W., DOBSON, C. M., SAUER, M. & KAMINSKI, C. F. (2011). In situ measurements of the formation and morphology of intracellular β -amyloid fibrils by super-resolution fluorescence imaging. *Journal of the American Chemical Society* **133**, 12902–12905.
- LEE, S., DESPLATS, P., LEE, H., SPENCER, B. & MASLIAH, E. (2012). Cell-to-cell transmission of α -synuclein aggregates. *Amyloid Proteins: Methods and Protocols, Methods in Molecular Biology* **849**, 347–361.
- LESNÉ, S., KOH, M. T., KOTILINEK, L., KAYED, R., GLABE, C. G., YANG, A., GALLAGHER, M. & ASHE, K. H. (2006). A specific amyloid- β protein assembly in the brain impairs memory. *Nature* **440**, 352–357.
- LORENZEN, N., COHEN, S. I. A., NIELSEN, S. B., HERLING, T. W., CHRISTIANSEN, G., DOBSON, C. M., KNOWLES, T. P. J. & OTZEN, D. (2012). Role of elongation and secondary pathways in S6 amyloid fibril growth. *Biophysical Journal* **102**, 2167–2175.
- MEISL, G., KIRKEGAARD, J. B., AROSIO, P., MICHAELS, T. C., VENDRUSCOLO, M., DOBSON, C. M., LINSE, S. & KNOWLES, T. P. J. (2016a). Molecular mechanisms of protein aggregation from global fitting of kinetic models. *Nature Protocols* **11**, 252–272.
- MEISL, G., YANG, X., FROHM, B., KNOWLES, T. P. J. & LINSE, S. (2016b). Quantitative analysis of intrinsic and extrinsic factors in the aggregation mechanism of Alzheimer-associated $A\beta$ -peptide. *Scientific Reports* **6**, 18728.
- MEISL, G., YANG, X., HELLSTRAND, E., FROHM, B., KIRKEGAARD, J. B., COHEN, S. I. A., DOBSON, C. M., LINSE, S. & KNOWLES, T. P. J. (2014). Differences in nucleation behavior underlie the contrasting aggregating kinetics of the $A\beta$ 40 and $A\beta$ 42 peptides. *Proceedings of the National Academy of Sciences of the United States of America* **111**, 9384–9389.
- MICHAELS, T. C. T., YDE, P., WILLIS, J. C. W., JENSEN, M. H., OTZEN, D., DOBSON, C. M., BUELL, A. K. & KNOWLES, T. P. J. (2015). The length distribution of frangible biofilaments. *The Journal of Chemical Physics* **143**, 164901.
- MUNISHKINA, L. A., HENRIQUES, J., UVERSKY, V. N. & FINK, A. L. (2004). Role of protein-water interactions and electrostatics in α -synuclein fibril formation. *Biochemistry* **43**, 3289–3300.
- NASIR, I., LINSE, S. & CABALEIRO-LAGO, C. (2015). Fluorescent filter-trap assay for amyloid fibril formation kinetics in complex solutions. *ACS Chemical Neuroscience* **6**, 1436–1444.
- OOSAWA, F. & ASAKURA, S. (1975). *Thermodynamics of the Polymerization of Protein*. Waltham, MA: Academic Press.
- PADRICK, S. B. & MIRANKER, A. D. (2002). Islet amyloid: phase partitioning and secondary nucleation are central to the mechanism of fibrillogenesis. *Biochemistry* **41**, 4694–4703.
- PINOTSI, D., BUELL, A. K., GALVAGNION, C., DOBSON, C. M., SCHIERLE, G. S. K. & KAMINSKI, C. F. (2014). Direct observation of heterogeneous amyloid fibril growth kinetics via two-color super-resolution microscopy. *Nano Letters* **14**, 339–345.
- PINOTSI, D., MICHEL, C. H., BUELL, A. K., LAINE, R. F., MAHOU, P., DOBSON, C. M., KAMINSKI, C. F. & SCHIERLE, G. S. K. (2016). Nanoscopic insights into seeding mechanisms and toxicity of α -synuclein species in neurons. *Proceedings of the National Academy of Sciences of the United States of America* **113**, 3815–3819.
- RABE, M., SORAGNI, A., REYNOLDS, N. P., VERDES, D., LIVERANI, E., RIEK, R. & SEEGER, S. (2013). On-surface aggregation of α -synuclein at nanomolar concentrations results in two distinct growth mechanisms. *ACS Chemical Neuroscience* **4**, 408–417.
- SCHULZ-SCHAEFFER, W. J. (2010). The synaptic pathology of α -synuclein aggregation in dementia with Lewy bodies, Parkinson's disease and Parkinson's disease dementia. *Acta Neuropathologica* **120**, 131–143.
- SHANKAR, G. M., LI, S., MEHTA, T. H., GARCIA-MUNOZ, A., SHEPARDSON, N. E., SMITH, I., BRETT, F. M., FARRELL, M. A., ROWAN, M. J., LEMERE, C. A., REGAN, C. M., WALSH, D. M., SABATINI, B. L. & SELKOE, D. J. (2008). Amyloid- β protein dimers isolated directly from Alzheimer's brains impair synaptic plasticity and memory. *Natural Medicines* **14**, 837–842.
- STEFANIS, L. (2012). α -Synuclein in Parkinson's disease. *Cold Spring Harbor Perspectives in Medicine* **4**, a009399.
- TANAKA, M., COLLINS, S. R., TOYAMA, B. H. & WEISSMAN, J. S. (2006). The physical basis of how prion conformations determine strain phenotypes. *Nature* **442**, 585–589.



- UVERSKY, V. N., LI, J. & FINK, A. L. (2001). Evidence for a partially folded intermediate in α -synuclein formation. *Journal of Biological Chemistry* **276**, 10737–10744.
- VÁCHA, R., LINSE, S. & LUND, M. (2014). Surface effects on aggregation kinetics of amyloidogenic peptides. *Journal of the American Chemical Society* **136**, 11776–11782.
- WAKABAYASHI, K., TANJI, K., MORI, F. & TAKAHASHI, H. (2007). The Lewy body in Parkinson's disease: molecules implicated in the formation and degradation of α -synuclein aggregates. *Neuropathology* **27**, 494–506.
- WINNER, B., JAPPELLI, R., MAJI, S. K., DESPLATS, P. A., BOYER, L., AIGNER, S., HETZER, C., LOHER, T., VILAR, M., CAMPIONI, S., TZITZILONIS, C., SORAGNI, A., JESSBERGER, S., MIRA, H., CONSIGLIO, A., PHAM, E., MASLIAH, E., GAGE, F. H. & RIEK, R. (2011). *In vivo* demonstration that α -synuclein oligomers are toxic. *Proceedings of the National Academy of Sciences of the United States of America* **108**, 4194–4199.
- WOLTER, S., LÖSCHBERGER, A., HOLM, T., AUFMKOLK, S., DABAUVALLE, M., VAN DE LINDE, S. & SAUER, M. (2012). rapidSTORM: accurate, fast open-source software for localization microscopy. *Nature Methods* **9**, 1040–1041.
- XUE, W., HELLEWELL, A. L., GOSAL, W. S., HOMANS, S. W., HEWITT, E. W. & RADFORD, S. E. (2009). Fibril fragmentation enhances amyloid cytotoxicity. *Journal of Biological Chemistry* **284**, 34272–34282.